arXiv:1609.05390v3 [astro-ph.SR] 13 Oct 2016

Evidence for a systematic offset of −0.25 mas in the *Gaia* DR1 parallaxes

Keivan G. Stassun[1,2] and Guillermo Torres[3]

ABSTRACT

We test the parallaxes reported in the *Gaia* first data release using the sample of eclipsing binaries with accurate, empirical distances from Stassun & Torres (2016). We find an average offset of -0.25 ± 0.05 mas in the sense of the *Gaia* parallaxes being too small (i.e., the distances too long). The offset does not depend strongly on obvious parameters such as color or brightness. However, we find with high confidence that the offset may depend on ecliptic latitude: the mean offset is -0.38 ± 0.06 mas in the ecliptic north and -0.05 ± 0.09 mas in the ecliptic south. The ecliptic latitude dependence may also be represented by the linear relation, $\Delta\pi \approx -0.22(\pm0.05) - 0.003(\pm0.001)\times\beta$ mas (β in degrees). Finally, there is a possible dependence of the parallax offset on distance, with the offset becoming negligible for $\pi \lesssim 1$ mas; we discuss whether this could be caused by a systematic error in the eclipsing binary distance scale, and reject this interpretation as unlikely.

1. Introduction

The advent of trigonometric parallaxes for $\sim10^9$ stars from the *Gaia* mission promises to revolutionize many areas of stellar and Galactic astrophysics, including exoplanet science. For example, with eventual expected precision in the parallax of $\approx$20 μas for bright exoplanet host stars, it should be possible to determine the stellar and planet radii and masses directly and empirically with accuracies of 3–5% (see, e.g., Stassun, Collins, & Gaudi 2016). Already, the *Gaia* first data release (DR1; Gaia Collaboration 2016) provides parallaxes for $\sim$2 million *Tycho-2* stars (the TGAS stars) with a nominal precision of $\approx$0.3 mas and with a quoted systematic uncertainty at present of 0.3 mas.

The results from DR1 are based on only 14 months of observations, and use external information in the form of earlier positions from the *Hipparcos* (ESA 1997; van Leeuwen 2007) and *Tycho-2* (Høg et al. 2000) catalogs to help remove degeneracies (the *Tycho-Gaia* Astrometric Solution; Michalik et al. 2015). Additionally, they rely on very provisional and as yet incomplete calibrations, and as a result the astrometric products including the parallaxes are still preliminary. Nonetheless, the new parallaxes represent such an improvement in both quality and quantity that they are certain to be used by the community for a wide range of astrophysical applications, at least until future *Gaia* releases supersede them.

It is essential, therefore, to assess the on-sky delivered performance of these parallaxes from *Gaia* DR1, especially the presence of any unexpected biases. This is particularly important in light of the experience from *Hipparcos*, which suffered a significant bias in at least the case of the Pleiades cluster (e.g., Pinsonneault et al. 1998). Such a check requires a set of benchmark stars whose parallaxes are determined independently and with an accuracy that is at least as good as that expected from *Gaia* DR1.

[1]Vanderbilt University, Department of Physics & Astronomy, 6301 Stevenson Center Ln., Nashville, TN 37235, USA; keivan.stassun@vanderbilt.edu

[2]Fisk University, Department of Physics, 1000 17th Ave. N., Nashville, TN 37208, USA

[3]Harvard-Smithsonian Center for Astrophysics, 60 Garden St., Cambridge, MA 02138, USA

Stassun & Torres (2016) assembled a sample of 158 eclipsing binary stars (EBs) whose radii and effective temperatures are known empirically and precisely, such that their bolometric luminosities are determined to high precision (via the Stefan-Boltzmann relation) and therefore independent of assumed distance. Stassun & Torres (2016) reported new, accurate measurements of the bolometric fluxes for these EBs which, together with the precisely known bolometric luminosities, yields a highly precise distance (or parallax). The precision of the parallaxes for this EB sample was predicted by Stassun & Torres (2016) to be ≈190 μas on average. This is a factor of ∼1.5 better than the median precision of 320 μas for *Gaia* DR1 (Gaia Collaboration 2016). It is even somewhat superior to the expected *Gaia* DR1 precision floor of 240 μas. These EB parallaxes can therefore readily serve as distance benchmarks for the trigonometric parallaxes reported by *Gaia* DR1, and in particular can be used to assess the presence of any systematics.

In this Letter, we report the results of testing the *Gaia* DR1 parallaxes against the Stassun & Torres (2016) EB benchmark sample. Section 2 describes the EB and *Gaia* data used. Section 3 presents the key result of a systematic offset in the *Gaia* parallaxes relative to the EB sample. Section 4 considers potential trends in the parallax offset with other parameters. Section 5 concludes with a summary of our conclusions.

2. Data

We adopted the predicted parallaxes for the 158 EBs included in the study of Stassun & Torres (2016). Of these, 116 had parallaxes available in the *Gaia* first data release. We excluded from our analysis any EBs identified as potentially problematic in Stassun & Torres (2016). This left 111 EBs with good parallaxes from both the EB analysis and from *Gaia*. These EBs are all relatively nearby, with parallaxes in the range $\pi \approx 0.3$–30 mas. The EBs and their relevant data are provided in Table 1.

3. Results

Figure 1 shows the direct comparison of the EB parallax predictions from Stassun & Torres (2016) versus the *Gaia* DR1 parallaxes for the study sample. The least-squares linear best fit, weighted by the measurement uncertainties in both quantities (Press et al. 1992), is $\pi_{\rm EB} = 0.08(\pm0.07) + 1.03(\pm0.01) \times \pi_{\rm Gaia}$. While this indicates a good 1-to-1 agreement to first order, the coefficient of 1.03±0.01 could be interpreted as a modest global difference of *scale* in the *Gaia* parallaxes relative to the EB parallaxes. However, considering all of the available evidence instead suggests a small *offset* in the *Gaia* parallaxes as we now discuss.

Figure 2 presents the overall distribution of parallax differences in the sense of $\pi_{\rm Gaia} - \pi_{\rm EB}$. The distribution appears roughly symmetric and normally distributed, with perhaps a sharper peak and more extended wings than a Gaussian, and there is a clear offset relative to zero. The mean offset is $\Delta\pi = -0.264 \pm 0.050$ mas, where the quoted error is the uncertainty of the mean for 111 measurements.

Stassun & Torres (2016) noted that a number of the EBs used in that study are known triple or quadruple systems. In general these companions contribute very little to the total system light, and Stassun & Torres (2016) found no evidence for significant systematics in their predicted parallaxes. Nonetheless, the offset that we find above for the *Gaia* parallaxes is small and could potentially have gone unnoticed in Stassun & Torres (2016). Indeed, the effect of additional light contribution to the EBs by companions would be in the sense of making the EB stars appear brighter, therefore inferred to be closer, and in turn the *Gaia* distances interpreted as too long (parallax too small).

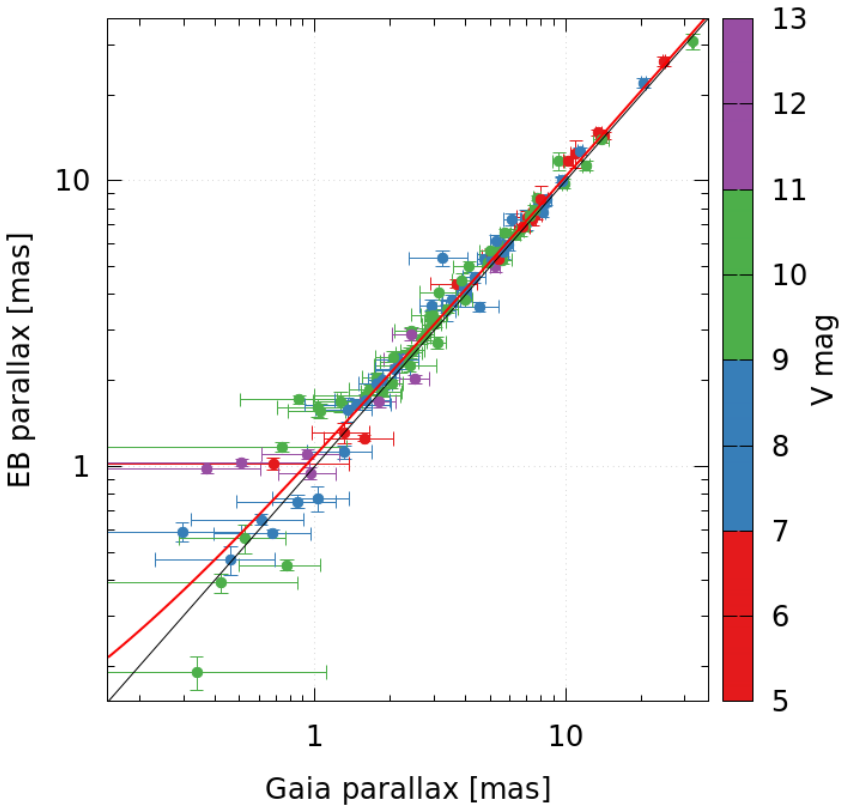

Fig. 1.— Direct comparison of predicted parallaxes from the eclipsing binary sample of Stassun & Torres (2016) versus the parallaxes from the *Gaia* first data release. The one-to-one line is shown in black and a least-squares linear best fit is shown in red.

In *Gaia* DR1, 12 of our EBs have known companions (see Table 1; one additional EB with a known companion is already excluded by the cuts discussed in Sec. 2). These EBs are indicated in blue in Fig. 2, which shows the two largest outliers to be triples. Excluding all of the triples results in a parallax offset of $\Delta\pi = -0.233 \pm 0.046$ mas, consistent with that determined for the full sample, though slightly smaller.

Overall, from the EB sample, a systematic offset in the *Gaia* DR1 parallaxes of -0.233 to -0.264 mas is indicated. For simplicity, we adopt the rounded value between these estimates of -0.25 ± 0.05 mas.

4. Discussion

The official *Gaia* DR1 documentation states: "There are colour dependent and spatially correlated systematic errors at the level of ± 0.2 mas. Over large spatial scales, the parallax zero-point variations reach an amplitude of ± 0.3 mas.... Furthermore, averaging parallaxes over small regions of the sky will not reduce the uncertainty on the mean below the 0.3 mas level.[1]" Our finding of a mean parallax offset

[1] http://www.cosmos.esa.int/web/gaia/dr1

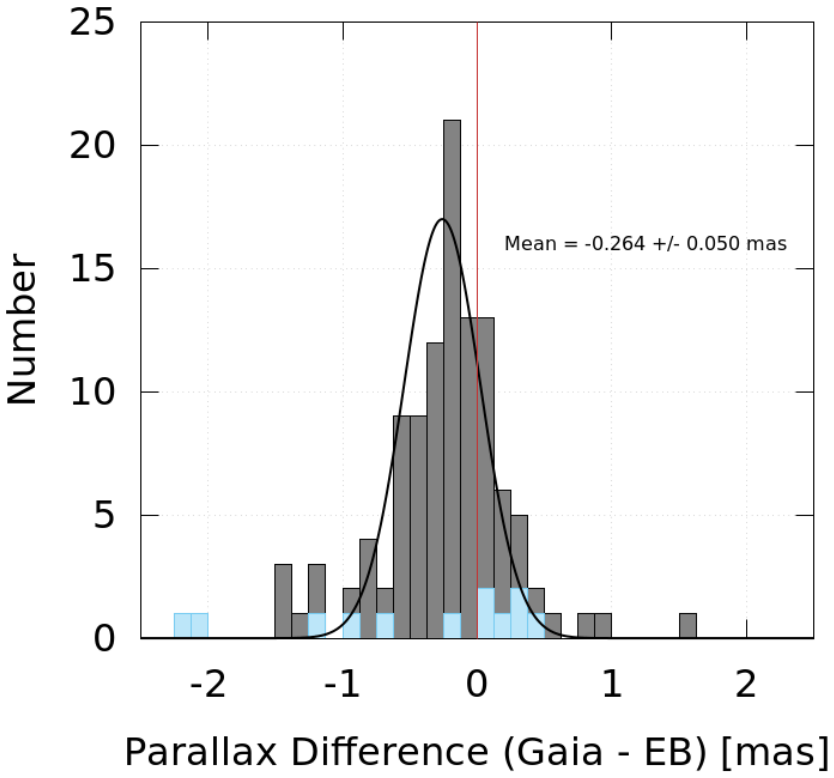

Fig. 2.— Distribution of $\Delta\pi$ (*Gaia*−EB). EBs with known tertiary companions are represented in blue. We find an offset of $\Delta\pi = -0.264 \pm 0.050$ mas for the entire sample and $\Delta\pi = -0.233 \pm 0.046$ mas when the triple systems are excluded. Also shown is a best-fit Gaussian with $\sigma^2 = \sigma^2_{\rm Gaia} + \sigma^2_{\rm EB}$, representing the quadrature sum of the typical random uncertainties from the *Gaia* and EB parallaxes; see Sec. 1.

of $\Delta\pi \approx -0.25 \pm 0.05$ mas (Sec. 3; Fig. 2) corroborates this statement, and further quantifies it using an independent benchmark sample of EBs with accurately known distances (Stassun & Torres 2016).

In principle this offset could be due to systematics in one or more of the EB parameters from which the EB distances are determined. If so, one might especially suspect the EB $T_{\rm eff}$ values: unlike the stellar radii, for example, which are determined from simple geometry, the $T_{\rm eff}$ values are determined from spectral analysis and/or spectral typing and/or color relations. The slope of the fitted relation in Fig. 1 would imply an error in the EB distance scale of ∼3%, which in turn would require a systematic error in $T_{\rm eff}$ of ∼1.5% (because $d \sim L_{\rm bol}^{1/2} \sim T_{\rm eff}^2$) or ∼105 K given the typical $T_{\rm eff}$ of the EB sample. The sense of the offset is that the EBs would have to be systematically too cool.

However, we do not consider this to be a likely possibility, for multiple reasons. First, Stassun & Torres (2016) found no evidence for a systematic offset of the EB parallaxes relative to the *Hipparcos* parallaxes which, even at the somewhat poorer precision of ∼1 mas, should have been apparent. Lindegren et al. (2016) compare the *Gaia* DR1 parallaxes against ∼87,000 *Hipparcos* stars in common, finding a statistically significant average offset just under −0.1 mas, smaller than, but in the same sense as the offset we find among our EB sample. Second, while systematics among various $T_{\rm eff}$ scales can be of order 100 K (see, e.g., Casagrande et al. 2011; Heiter et al. 2015), it is unlikely that they should produce a net offset of this

entire magnitude in a sample of 111 EBs spanning a large range of $T_{\rm eff}$, given the different methodologies and calibrations adopted by the various authors. Finally, we have directly examined the degree to which $\Delta\pi$ might correlate with $T_{\rm eff}$ in the EB sample (Fig. 3, upper right), finding very weak evidence for a correlation: The regression relation has a coefficient of determination $R^2 = 0.13$; this parameter explains only 13% of the variance in $\Delta\pi$. Indeed, a Kendall's τ non-parametric correlation test gives a probability of 51% that $\Delta\pi$ and $T_{\rm eff}$ are uncorrelated. (We checked that the parallax *ratio* versus $T_{\rm eff}$ is also not significantly correlated.) Incidentally, this also suggests little to no dependence of $\Delta\pi$ with color, since $T_{\rm eff}$ can be taken as a proxy for color.

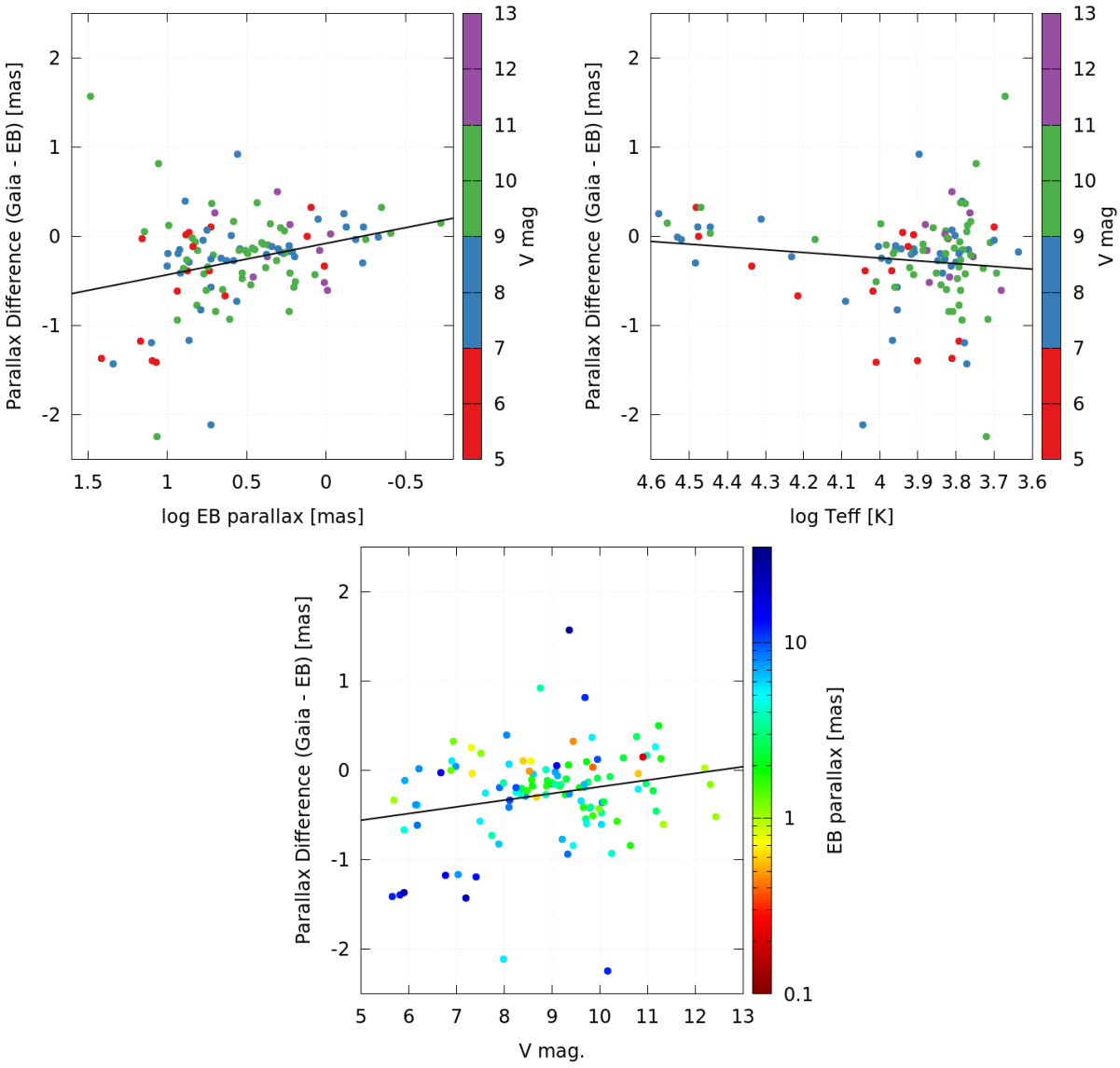

Fig. 3.— Potential correlations between $\Delta\pi$ and $\pi_{\rm EB}$, EB $\log T_{\rm eff}$, and V mag. Best fitting linear regression lines are shown for each (see the text).

With a current sample of 111 EBs that overlap with the *Gaia* DR1 parallaxes, it is difficult to ascertain

with certainty whether any higher-order dependencies are at work beyond a simple offset. Nonetheless, it is possible that the parallax offset we observe is a function of one or more parameters. We have considered some obvious possible parameters, including distance, and brightness. These are represented in Figure 3. There is some evidence for a dependence of $\Delta\pi$ on distance and/or brightness, however it is difficult to gauge whether these modest distance and brightness dependencies are independent of one another. A priori, a possible dependence on brightness may be more likely than a dependence on distance: because of the manner in which the trigonometric parallax measurements are made (linear offsets on the detector), they are more likely to depend on parameters that affect the displacement calibration (e.g., color or brightness) than the displacement itself. Thus there is not strong evidence for a dependence of the offset with brightness or color, at least in our sample.

The apparent correlation of $\Delta\pi$ with π may be a consequence of the tendency for the EBs with the largest π to be located in the ecliptic north, where we find the largest overall offset (see below). In any event, among our 12 EBs with $\pi < 1$ mas, the average offset is $\Delta\pi = 0.00 \pm 0.07$ mas. Thus, it appears that the offset vanishes for very small parallaxes, $\pi \lesssim 1$ mas. This would be consistent with the findings of Lindegren et al. (2016) and also Casertano et al. (2016), who find good agreement with the *Gaia* DR1 parallaxes in separate samples of very distant Cepheids with estimates based on period-luminosity relations. Casertano et al. (2016) also find evidence for a parallax offset, in the same sense as we find, among the small number of very nearby, bright Cepheids in their sample.

Finally, we have considered the possible spatial dependence of $\Delta\pi$. There is evidence for a trend or difference by ecliptic latitude (Fig. 4). The mean parallax offset for EBs in the northern ecliptic hemisphere is statistically significant with $\Delta\pi = -0.38 \pm 0.06$ mas, whereas in the southern ecliptic hemisphere it is not significant with $\Delta\pi = -0.05 \pm 0.09$ mas. A two-sided Kolmogorov-Smirnov test gives a probability of 0.0001 that this difference could occur by chance. Alternatively, the trend can be represented as a linear variation with latitude, $\Delta\pi \approx -0.22(\pm 0.05) - 0.003(\pm 0.001) \times \beta$ mas (β in degrees). A Kendall's τ test indicates that the correlation between parallax offset and ecliptic latitude is significant with 99.7% confidence.

The possibility that systematics in the *Gaia* DR1 parallaxes are dependent on ecliptic latitude was suggested in the *Gaia* documentation (Lindegren et al. 2016). These authors reported that a comparison with parallaxes from the *Hipparcos* mission indicates an overall statistically significant offset $\Delta\pi = -0.089 \pm 0.006$ mas, the *Gaia* values being smaller, but that the northern ecliptic hemisphere shows a larger offset of -0.130 ± 0.006 mas compared to the southern hemisphere (-0.053 ± 0.006 mas).

5. Summary and Conclusions

Here we present evidence of a small but systematic offset in the average zero-point of the parallax measurements recently released by the *Gaia* Mission of about -0.25 ± 0.05 mas, in the sense that the *Gaia* values are too small. We also find evidence to suggest that the offset is a function of ecliptic latitude. The offset in the northern ecliptic hemisphere is -0.38 ± 0.06 mas and -0.05 ± 0.09 mas in the southern ecliptic hemisphere. Alternatively, the offset may also be represented as a linear function of the ecliptic latitude, β (°), according to $\Delta\pi \approx -0.22(\pm 0.05) - 0.003(\pm 0.001) \times \beta$ mas.

To apply the correction, this (negative) offset must be *subtracted* from the reported *Gaia* DR1 parallaxes. At present we can only confirm that the offset is statistically valid for relatively large parallaxes, $\pi \gtrsim 1$ mas.

The reference for this determination is a set of more than 100 independently inferred parallaxes from a

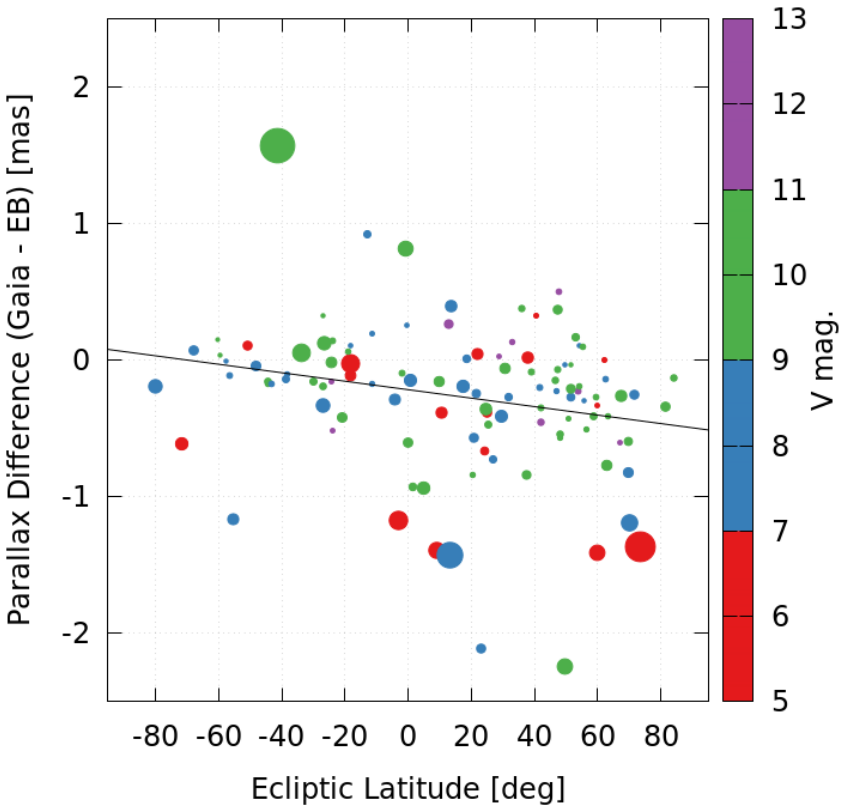

Fig. 4.— Parallax differences as a function of ecliptic latitude. A trend is found (black line) with 99.7% confidence, which may also be interpreted as a significant difference in the ecliptic north ($\Delta\pi = -0.38 \pm 0.06$ mas) but not in the ecliptic south ($\Delta\pi = -0.05 \pm 0.09$ mas). Color represents EB brightness and symbol size is proportional to π.

benchmark sample of well-studied eclipsing binaries with a wide range of brightnesses and distributed over the entire sky. This paper presents evidence of a *difference* between the *Gaia* and EB parallaxes, which we have interpreted here as a systematic error in *Gaia* after discussing the alternative. In particular, we have considered the possibility of a systematic offset in the EB effective temperature scale as a possible, but unlikely alternative explanation.

It is expected that future releases of the *Gaia* catalog will remove this small shift as the number of observations increases, calibrations are improved, and the astrometric solution transitions to a self-consistent global fit using only *Gaia* data, independent of external astrometric information. Indeed, these final trigonometric parallaxes may then be used to further refine the EB sample itself, such as improvements to the EB effective temperature scale. In the meantime, investigators using the parallax results from *Gaia* DR1 are encouraged to keep the systematic error reported here in mind.

This work has made use of the Filtergraph data visualization service at `filtergraph.vanderbilt.edu` (Burger et al. 2013). K.G.S. acknowledges partial support from NSF PAARE grant AST-1358862. G.T. acknowledges partial support for this work from NSF grant AST-1509375. The authors are grateful to

S. Casertano and A. Riess for sharing their results in advance of publication. We are grateful to the referee for critiques and suggestions that improved the manuscript. This work has made use of data from the European Space Agency (ESA) mission *Gaia* (http://www.cosmos.esa.int/gaia), processed by the *Gaia* Data Processing and Analysis Consortium (DPAC, http://www.cosmos.esa.int/web/gaia/dpac/consortium). Funding for the DPAC has been provided by national institutions, in particular the institutions participating in the *Gaia* Multilateral Agreement.

REFERENCES

Burger, D., Stassun, K. G., Pepper, J., et al. 2013, Astronomy and Computing, 2, 40

Casagrande, L., Schönrich, R., Asplund, M., et al. 2011, A&A, 530, A138

Casertano, S., Riess, A. G., Bucciarelli, B., & Lattanzi, M. G. 2016, arXiv:1609.05175

ESA Special Publication, Vol. 1200, The HIPPARCOS and TYCHO catalogs. Astrometric and photometric star catalogues derived from the ESA HIPPARCOS Space Astrometry Mission

A. G. A. Brown, A. Vallenari, T. Prusti, J. H. de Bruijne, F. Mignard, et al. 2016, A&A, special Gaia volume

Heiter, U., Jofré, P., Gustafsson, B., et al. 2015, A&A, 582, A49

Høg, E., Fabricius, C., Makarov, V. V., et al. 2000, A&A, 355, L27

Lindegren, L., Lammers, U., Bastian, U. et al. 2016, A&A, in press (arXiv:1609.04303)

Michalik, D., Lindegren, L., & Hobbs, D. 2015, A&A, 574, A115

Pinsonneault, M. H., Stauffer, J., Soderblom, D. R., King, J. R., & Hanson, R. B. 1998, ApJ, 504, 170

Press, W. H., Teukolsky, S. A., Vetterling, W. T., & Flannery, B. P. 1992, Cambridge: University Press, —c1992, 2nd ed.,

Stassun, K. G., & Torres, G. 2016, AJ, in press (arXiv:1609.02579)

Stassun, K. G., Collins, K. A., & Gaudi, B. S. 2016, AJ, submitted (arXiv:1609.04389)

van Leeuwen, F. 2007, Astrophysics and Space Science Library, 350

This preprint was prepared with the AAS LaTeX macros v5.2.

Table 1. Eclipsing Binary and *Gaia* Data

Name	Tycho	$T_{\rm eff}$[a] K	$\sigma_{T_{\rm eff}}$ K	V mag.	χ^2_ν[b]	$\pi_{\rm EB}$ mas	$+\sigma_{\pi_{\rm EB}}$ mas	$-\sigma_{\pi_{\rm EB}}$ mas	$\pi_{\rm Gaia}$ mas	$\sigma_{\pi_{\rm Gaia}}$ mas	RA deg.	Dec. deg.
UV Psc[c]	0026-0577-1	5780	100	9.01	2.72	12.47	0.57	0.53	14.392	0.407	19.2297	6.8117
XY Cet	0051-0832-1	7870	115	8.75	1.6	3.62	0.14	0.13	4.542	0.891	44.8897	3.5176
V1130 Tau	0066-1108-1	6625	70	6.66	1.34	14.35	0.36	0.37	14.329	0.332	57.6748	1.5639
EW Ori	0104-1206-1	5970	100	9.78	0.71	5.9	0.22	0.21	5.482	0.233	80.0381	2.0444
U Oph[d]	0400-1862-1	16440	250	5.9	1.15	4.35	0.14	0.17	3.685	0.775	259.1322	1.2105

Note. — Table 1 is published in its entirety in machine-readable format. A portion is shown here for guidance regarding its form and content.

[a]Effective temperature for the primary component.

[b]χ^2_ν of SED fit from Stassun & Torres (2016). Stars with $\chi^2_\nu > 20$ were considered unacceptable and are excluded from analysis in this paper also.

[c]Flagged in Stassun & Torres (2016) as a large outlier relative to *Hipparcos* and excluded from analysis in this paper.

[d]Identified in Stassun & Torres (2016) as a known triple system; these are retained in the analysis in this paper (see the text).

Table 1. Eclipsing Binary and *Gaia* Data

Name	Tycho	$T_{\rm eff}$[a] K	$\sigma_{T_{\rm eff}}$ K	V mag.	χ^{2}_{ν}[b]	$\pi_{\rm EB}$ mas	$+\sigma_{\pi_{\rm EB}}$ mas	$-\sigma_{\pi_{\rm EB}}$ mas	$\pi_{\rm Gaia}$ mas	$\sigma_{\pi_{\rm Gaia}}$ mas	RA deg.	Dec. deg.
UV Psc[c]	0026-0577-1	5780	100	9.01	2.72	12.47	0.57	0.53	14.392	0.407	19.22966316	6.8116994
XY Cet	0051-0832-1	7870	115	8.75	1.6	3.62	0.14	0.13	4.542	0.891	44.88971498	3.51756508
V1130 Tau	0066-1108-1	6625	70	6.66	1.34	14.35	0.36	0.37	14.329	0.332	57.67475441	1.56394837
EW Ori	0104-1206-1	5970	100	9.78	0.71	5.9	0.22	0.21	5.482	0.233	80.0381137	2.0444353
V578 Mon	0154-2528-1	30000	740	8.55	0.65	0.75	0.04	0.04	0.855	0.364	98.0025408	4.8780283
AI Hya	0196-0626-1	6700	60	9.35	7.02	1.82	0.07	0.07	1.879	0.353	124.697754	0.283378
FM Leo	0263-0727-1	6316	240	8.45	3.49	7.29	0.64	0.57	7.004	0.322	168.18789591	0.34800926
AQ Ser	0340-0588-1	6430	100	10.65	1.89	1.71	0.06	0.06	0.869	0.366	230.5632692	2.50308
V335 Ser	0353-0301-1	9020	150	7.49	1.99	5.31	0.2	0.21	4.742	0.302	239.7739821	0.5957072
U Oph[d]	0400-1862-1	16440	250	5.9	1.15	4.35	0.14	0.17	3.685	0.775	259.13215193	1.21054491
V2368 Oph	0404-2156-1	9300	200	6.18	2.84	5.44	0.32	0.29	5.06	0.428	259.05941952	2.18620241
V413 Ser[d]	0446-0091-1	11100	300	7.99	1.64	5.34	0.35	0.32	3.23	0.853	278.78422403	0.04301045
CoRoT 105906206	0459-0892-1	6750	150	12.21	1.8	0.94	0.05	0.04	0.964	0.249	280.820621	5.966736
IO Aqr[d]	0511-0960-1	6336	125	8.86	0.87	3.97	0.18	0.17	3.979	0.246	310.18946139	0.93917186
V1388 Ori	0738-0244-1	20500	500	7.5	3.28	1.12	0.06	0.06	1.315	0.381	92.74652296	11.99485667
WZ Oph	0977-0216-1	6165	100	9.12	3.6	6.67	0.27	0.27	6.608	0.238	256.66267585	7.78271678
V2365 Oph	0977-0547-1	9500	200	8.86	1.68	3.81	0.19	0.16	3.542	0.29	257.19075987	9.1861524
V624 Her	1005-2131-1	8150	150	6.2	2.11	7.6	0.29	0.35	7.615	0.489	266.07186051	14.41006621
EE Peg[d]	1120-0161-1	8700	200	6.98	1.72	7.33	0.41	0.32	7.372	0.298	325.00784071	9.18475409
CF Tau[d]	1262-0050-1	5200	150	10.24	1.31	4.06	0.26	0.25	3.132	0.513	61.2922271	22.4967133
V1094 Tau	1263-0642-1	5850	100	8.97	0.74	8.4	0.34	0.3	8.256	0.251	63.0149692	21.9473753
CD Tau[d]	1291-0292-1	6200	50	6.77	4.36	14.73	0.41	0.39	13.559	0.375	79.379796	20.131842
FT Ori	1326-0910-1	9600	400	9.29	7.62	2.32	0.22	0.19	2.222	0.383	93.4923067	21.4275506
BP Vul	1644-2113-1	7715	150	9.95	2.61	2.49	0.11	0.1	2.402	0.294	306.38853349	21.0383264
AD Boo	2015-0216-1	6575	120	9.44	2.31	4.99	0.2	0.19	4.146	0.554	218.8032496	24.6392644
RT CrB	2039-1337-1	5134	100	10.22	1.84	2.54	0.11	0.11	2.475	0.268	234.5126246	29.48720441
LV Her	2076-1042-1	6060	150	10.97	1.17	2.82	0.16	0.15	2.675	0.243	263.8850083	23.1751667
DI Her	2109-0775-1	17000	800	8.47	0.65	1.58	0.16	0.15	1.354	0.346	283.35933236	24.27799733
BK Peg	2254-2563-1	6265	85	10.04	0.82	3.38	0.11	0.1	2.911	0.482	356.7852704	26.5666433
AR Aur	2398-1311-1	10950	300	6.14	1.83	7.43	0.43	0.41	7.047	0.611	79.57875162	33.76734788
HP Aur[d]	2401-1263-1	5810	120	11.17	1.31	5.01	0.23	0.21	5.273	0.22	77.590762	35.796286
V432 Aur	2416-0768-1	6080	85	8.05	4.61	7.72	0.29	0.28	8.118	0.255	84.38545384	37.08673876
WW Aur	2426-0345-1	7960	420	5.82	3.06	12.42	1.46	1.26	11.026	0.5	98.11326959	32.45489819
KX Cnc	2484-0592-1	5900	100	7.19	1.05	21.97	0.83	0.77	20.542	0.378	130.69254478	31.86260197
HD 71636	2489-1972-1	6950	140	7.9	0.92	8.59	0.41	0.35	8.403	0.402	127.48463115	37.07096799
CV Boo	2570-0843-1	5760	150	10.99	1.64	3.83	0.23	0.21	3.997	0.253	231.5813963	36.9815092
V501 Her	2606-1905-1	5683	100	11.12	0.5	2.36	0.09	0.09	2.129	0.231	263.93108	30.64308
V885 Cyg	2655-1877-1	8150	150	9.99	2.27	1.17	0.05	0.04	0.744	0.608	293.2077342	30.0213972
MY Cyg	2680-1529-1	7050	200	8.34	1.79	4.22	0.27	0.25	3.952	0.235	305.01412547	33.94306105
V453 Cyg	2683-3326-1	27800	400	8.4	1.62	0.58	0.02	0.02	0.683	0.288	301.6456979	35.7406322
V442 Cyg	2685-1903-1	6900	100	9.7	1.68	2.98	0.1	0.09	2.44	0.346	306.9679333	30.791195

Table 1—Continued

Name	Tycho	$T_{\rm eff}$[a] K	$\sigma_{T_{\rm eff}}$ K	V mag.	χ^2_ν[b]	$\pi_{\rm EB}$ mas	$+\sigma_{\pi_{\rm EB}}$ mas	$-\sigma_{\pi_{\rm EB}}$ mas	$\pi_{\rm Gaia}$ mas	$\sigma_{\pi_{\rm Gaia}}$ mas	RA deg.	Dec. deg.
CG Cyg[d]	2696-2945-1	5260	180	10.16	3.26	11.68	0.89	0.8	9.438	0.545	314.556071	35.174911
Y Cyg	2696-3486-1	33200	600	7.32	1.58	0.65	0.03	0.03	0.613	0.291	313.01490655	34.65763334
KIC 8410637	3130-2385-1	4800	80	11.33	2.63	0.98	0.04	0.04	0.373	0.238	282.1587429	44.4860661
KIC 3858884	3135-0651-1	6800	70	9.28	10.6	2.05	0.07	0.07	1.776	0.224	293.69543217	38.98278969
V380 Cyg	3141-3692-1	21700	400	5.68	0.9	1.02	0.05	0.04	0.685	0.696	297.65553032	40.59976051
V478 Cyg	3151-2222-1	30479	1000	8.68	5.82	0.59	0.05	0.04	0.297	0.214	304.91144903	38.33588957
V364 Lac	3215-0971-1	8250	150	8.36	2.3	2.37	0.1	0.1	2.166	0.423	343.06170498	38.74573119
V342 And[d]	3246-2531-1	6200	100	7.82	24.15	12.15	0.69	0.69	4.915	0.333	2.5133037	46.3903136
CO And[d]	3268-0398-1	6140	130	10.77	1.34	2.71	0.13	0.13	3.087	0.274	17.8534604	46.9637042
V570 Per	3314-1225-1	6842	50	8.09	1.98	8.26	0.19	0.18	7.847	0.264	47.39559997	48.62463695
IM Per[d]	3323-1123-1	7580	150	11.28	3.91	1.68	0.09	0.07	1.814	0.291	47.9262975	52.2117222
IQ Per	3331-1175-1	12300	230	7.73	3.2	3.65	0.16	0.15	2.92	0.281	59.93615716	48.15124737
HS Aur	3394-0326-1	5350	75	10.05	1.71	7.89	0.3	0.29	7.53	0.282	102.82698688	47.67338091
FL Lyr	3542-1492-1	6150	100	9.36	1.53	7.51	0.33	0.29	7.25	0.217	288.02025709	46.32412867
V2080 Cyg	3551-1744-1	6000	75	7.4	2.15	12.63	0.36	0.35	11.439	0.252	291.69977628	50.14549388
KIC 9246715	3559-0102-1	4930	190	9.65	3.92	1.68	0.15	0.13	1.272	0.279	300.9513421	45.6041192
V1061 Cyg	3600-0472-1	6180	100	9.21	2.29	6.54	0.26	0.21	5.768	0.291	316.83549669	52.04956061
RW Lac	3629-0740-1	5760	100	10.81	1.83	5.15	0.21	0.2	4.942	0.301	341.2378975	49.6576586
AP And	3639-0915-1	6565	150	11.19	1.02	2.89	0.15	0.14	2.433	0.388	357.3779521	45.7892364
IT Cas	3650-0959-1	6470	100	11.23	1.13	2.02	0.07	0.07	2.52	0.339	355.5058137	51.7435558
V505 Per[c]	3690-0536-1	6510	50	6.88	0.99	16.93	0.41	0.37	15.563	0.323	35.30401536	54.51007761
V1143 Cyg	3938-1983-1	6450	100	5.9	2.02	26.11	0.96	0.88	24.746	0.354	294.6715988	54.97379118
RT And[c]	3998-2167-1	6100	150	9.04	5.42	9.17	0.54	0.5	10.053	0.225	347.79207917	53.02584476
V396 Cas	4006-1219-1	9225	150	9.58	1.82	1.85	0.08	0.06	1.661	0.279	348.3999133	56.7381106
PV Cas	4010-1411-1	10200	250	9.86	3.77	1.56	0.09	0.08	1.057	0.276	347.51073	59.2017072
MU Cas	4014-1119-1	14750	800	10.8	3.1	0.56	0.07	0.06	0.528	0.24	3.96483911	60.43156742
V459 Cas	4030-1001-1	9140	300	10.36	3.94	1.6	0.12	0.11	1.028	0.318	17.8746546	61.1466544
SZ Cam[d]	4068-1651-1	30320	150	6.93	3.57	1.25	0.03	0.03	1.578	0.484	61.95538446	62.33293757
WW Cam	4073-1191-1	8350	135	10.09	3.26	2.41	0.11	0.1	2.062	0.303	67.8553362	64.3626378
ZZ UMa	4144-0400-1	5960	70	9.83	1.74	5.27	0.15	0.14	5.638	0.469	157.5133057	61.81150639
WX Cep	4268-0138-1	8150	250	9	12.47	2.01	0.16	0.14	1.873	0.234	337.81577827	63.52265463
AH Cep	4273-0857-1	29900	1000	6.88	5.84	1.31	0.11	0.1	1.315	0.341	341.97059463	65.06216647
YZ Cas	4307-2167-1	10200	300	5.65	4.63	11.71	0.41	0.37	10.3	0.488	11.41282179	74.98807249
BF Dra	4435-1750-1	6360	150	9.76	1.42	2.9	0.16	0.13	2.77	0.224	282.74730236	69.88263435
UZ Dra	4444-1595-1	6200	100	9.6	4.95	5.55	0.24	0.23	5.206	0.253	291.4793554	68.9353192
EK Cep	4466-2120-1	9000	200	7.89	4.61	6.14	0.32	0.3	5.316	0.308	325.33960392	69.69280812
VZ Cep	4470-1334-1	6670	160	9.72	1.82	4.47	0.25	0.24	3.876	0.348	327.5463979	71.4439708
EY Cep	4521-0349-1	7090	150	9.81	0.77	3.37	0.16	0.15	2.957	0.314	55.0169708	81.0191858
AY Cam	4540-1742-1	7250	100	9.72	0.99	1.94	0.06	0.06	2.035	0.225	126.4657754	77.2185686
EI Cep	4599-0082-1	6750	100	7.61	1.93	5.32	0.2	0.17	5.066	0.243	322.11752646	76.40349679
GG Ori	4767-0857-1	9950	200	10.49	3.43	2.25	0.11	0.1	2.396	0.673	85.792592	−0.687461

Table 1—Continued

Name	Tycho	$T_{\rm eff}$ [a] K	$\sigma_{T_{\rm eff}}$ K	V mag.	χ^2_ν [b]	$\pi_{\rm EB}$ mas	$+\sigma_{\pi_{\rm EB}}$ mas	$-\sigma_{\pi_{\rm EB}}$ mas	$\pi_{\rm Gaia}$ mas	$\sigma_{\pi_{\rm Gaia}}$ mas	RA deg.	Dec. deg.
V530 Ori	4786-0571-1	5890	100	9.96	1.09	9.77	0.41	0.38	9.897	0.224	91.1408646	−3.1976719
V501 Mon	4799-1943-1	7510	100	12.32	2.48	1.1	0.04	0.04	0.939	0.325	100.173871	−1.111114
CoRoT 102918586	4800-1540-1	7400	90	12.43	0.99	1.03	0.03	0.03	0.513	0.443	102.226296	−0.873125
HI Mon	4809-0245-1	29500	600	9.45	4.1	0.45	0.02	0.02	0.776	0.274	103.9544438	−4.0432744
FS Mon	4825-2374-1	6715	100	9.68	2.17	3.13	0.1	0.1	2.937	0.261	111.1762621	−5.1540478
VZ Hya	4874-0811-1	6645	150	9.06	0.8	6.95	0.35	0.32	6.936	0.235	127.9225553	−6.31876784
IM Vir	4955-0912-1	5570	100	9.69	1.39	11.3	0.48	0.45	12.12	0.342	192.4112337	−6.0791283
BH Vir	4968-0569-1	6100	100	9.68	1.81	6.46	0.28	0.27	6.306	0.296	209.60358735	−1.66082075
EG Ser	5099-0149-1	9900	200	8.24	4.57	4.59	0.21	0.2	4.342	0.445	276.5091796	−1.6809489
LL Aqr	5236-0883-1	6080	45	9.32	0.9	8.68	0.19	0.19	7.746	0.271	338.67563291	−3.5994906
EF Aqr	5248-1030-1	6150	65	10.04	0.67	5.66	0.15	0.14	5.056	0.499	345.3295333	−6.4375969
PV Pup	5422-3294-1	6920	300	6.93	85.13	11.98	1.49	1.28	11.969	0.334	116.36971411	−14.68613454
GZ CMa	5965-0860-1	8800	350	7.98	2.25	3.5	0.32	0.28	3.36	0.311	109.08002714	−16.71669043
SW CMa	5976-0630-1	8200	150	9.16	3.87	1.77	0.07	0.08	1.596	0.601	107.06348559	−22.4403521
HW CMa	5976-1266-1	7700	150	9.18	2.14	3.21	0.15	0.14	3.056	0.305	107.0910854	−22.4082975
HS Hya	6069-1131-1	6500	50	8.12	1.04	10.01	0.23	0.16	9.676	0.268	156.15319885	−19.09248835
AK For	6446-0342-1	4690	100	9.36	5.68	30.65	1.88	1.8	32.222	0.247	52.34530926	−24.10085907
V3903 Sgr	6843-0543-1	38000	1900	7.31	0.47	0.77	0.08	0.07	1.029	0.348	272.32374524	−23.98839603
TZ For	7026-0633-1	5000	100	6.89	0.75	5.33	0.25	0.21	5.436	0.254	48.66705279	−35.55766586
HD 187669	7443-0867-1	4330	70	8.88	1.13	1.64	0.07	0.07	1.467	0.549	298.0920162	−32.5610378
PT Vel	7690-2859-1	9250	150	7.03	13.27	7.31	0.38	0.35	6.145	0.451	137.74049908	−43.26748036
V4089 Sgr	7936-2270-1	8433	97	5.91	2.66	6.86	0.18	0.18	6.748	0.489	293.53535674	−40.03463968
AI Phe	8032-0625-1	5010	120	8.6	0.52	5.98	0.31	0.3	5.938	0.238	17.39247871	−46.26558121
V467 Vel	8151-1072-1	36200	2500	10.9	10.29	0.19	0.03	0.02	0.339	0.777	130.95325	−46.125928
V636 Cen	8285-0847-1	5900	85	9.09	0.25	13.91	0.43	0.4	13.962	0.991	214.24130865	−49.94510016
TV Nor	8322-0334-1	9120	150	9.06	1.99	3.55	0.13	0.12	3.389	0.33	241.0385217	−51.5444425
GV Car	8627-1797-1	10100	300	8.91	2.72	2.19	0.17	0.13	2.075	0.325	166.387038	−58.730517
SZ Cen	8676-2330-1	8100	300	8.59	17.76	1.94	0.18	0.16	1.769	0.263	207.646219	−58.49919382
DW Car	8957-1314-1	27900	1000	9.85	3.76	0.39	0.03	0.03	0.423	0.432	160.79195	−60.0365947
EM Car	8959-0569-1	34000	2000	8.52	0.99	0.47	0.06	0.05	0.464	0.232	168.0187762	−61.0952586
V349 Ara	9038-0641-1	9074	200	8.58	3.91	1.7	0.09	0.09	1.6	0.392	249.8442192	−60.9617075
UX Men [d]	9378-0190-1	6200	100	8.24	1.15	9.91	0.39	0.38	9.718	0.214	82.51326739	−76.24870878
RZ Cha	9422-0104-1	6450	150	8.09	0.68	5.61	0.28	0.28	5.685	0.259	160.60043486	−82.0372742
TZ Men	9496-0590-1	10400	500	6.18	2.04	8.63	1.01	0.81	8.022	0.488	82.557857	−84.78510291

[a]Effective temperature for the primary component.

[b]χ^2_ν of spectral energy distribution fit from Stassun & Torres (2016). Stars with $\chi^2_\nu > 20$ were considered unacceptable and are excluded from analysis in this paper also.

[c]Flagged in Stassun & Torres (2016) as a large outlier relative to *Hipparcos* and excluded from analysis in this paper.

[d]Identified in Stassun & Torres (2016) as a known triple system; these are retained in the analysis in this paper but discussed separately in the text.